Zeitschrift: IABSE reports of the working commissions = Rapports des commissions de travail AIPC = IVBH Berichte der Arbeitskommissionen

Band: 13 (1973)

Artikel: Analytical and experimental studies on the deformation evaluation of reinforced concrete columns under seismic forces

Autor: Muguruma, Hiroshi / Tominaga, Megumi / Watanabe, Fumio

DOI: https://doi.org/10.5169/seals-13749

Analytical and Experimental Studies on the Deformation Evaluation of Reinforced Concrete Columns under Seismic Forces

Etudes analytiques et expérimentales sur l'évaluation de la déformation de colonnes en béton armé et précontraint soumises à des charges sismiques

Analytische und experimentelle Studie über die Deformationsabschätzung von Stahlbeton- und vorgespannten Stützen unter Erdbebenlasten

Hiroshi MUGURUMA
Professor of Architectural Engineering

Megumi TOMINAGA
Associate Professor of Architectural Engineering

Fumio WATANABE
Assistant Professor of Architectural Engineering

Japan

In the response analysis of middle or short height reinforced concrete structures, it is most important precisely to evaluate the stiffness degradation in the hysteresis loops because of their frequency sensitivity. It is supposed that these stiffness degradations are mainly caused by the shear deformation of reinforced concrete structural elements.

This study points out that the difficulties exists on the lack of the knowledges to estimate these shear deformations, such as the slippage of the reinforcing bars or shear cracks in the columns.

The authors proposed a research hypothesis that the deformation of the reinforced concrete columns under combined shear and flexure may be considered as the sum of individual deformation under the respective forces. The results of comprehensive experiments, including an elaborate measurement on the curvature distribution and the bond characteristics of reinforcing bars, gave a substantial support to this assumtion.

From the observed deformation mechanisms, a simple deformation model for the analytical purpose could be proposed. In this model the flexural deformation and the shear distortion may arise independently.

BASIC EXPERIMENTAL STUDY

Materials

River sand, synthetic lightweight coase aggregate (expanded shale) and portland cement were used. Mix proportion of concrete was 1:2.1:1.43 and water cement ratio, 51% by weight ratio respectively. Compressive strength of concrete at test was about 350 kg/cm^2 and the splitting tensile strength was about 19.7 kg/cm^2. Deformed bars of 19, 13, 10mm dia. (f_y = 4600 kg/cm^2) was used for longitudinal reinforcing steel and round bars of 6mm dia. (f_y = 2910 kg/cm^2) were used for the lateral reinforcing steel.

Specimens

Fig. 1 shows the details of test specimens. To obtain the necessary informations the following widely ranged properties were given to the tested columns.

1. Shear span ratio (a/D); 1.0, 2.0 and 3.0.
2. Amount of longitudinal reinforcement P_t; 1.9, 2.54 and 3.8% in area ratio of gross steel.
3. Amount of lateral shear reinforcement P_v; 0, 0.25, 0.37, 0.75 1.50% in area ratio.

Each specimen had a rectangular section BxD = 15cm x 20cm. The number and the diameters of the longitudinal reinforcements were intentionally chosen so as to yield the same total perimeter ψ = 24cm in both compressive and tensile zones of the column respectively.

Test method

Monotonous loading tests were performed for all kinds of the specimens and reversed repeated loading tests with constant amplitude of the member rotation R = ± 0.01 rad. were performed only for the specimens of F-series with P_t = 3.8% in three kinds of shear span ratios. For comparison pure flexural tests were also performed. Fig. 2 shows the overall loading devices. Axial load was maintained so as to yield net concrete stress fc'/6 during the test.

The curvature distribution were measured by the dial gages attached to the 6mm dia. bolts buried in the specimen at intervals of 10cm. The relative displacements over the story height 2a between inner loading points were recorded as the story deflection δ or the member rotation. Also the strain distributions of the longitudinal reinforcements were measured by the electric resistance wire strain gages.

Test results

Fig. 3 shows the crack appearance of test specimens at the ultimate stage under monotonous loading, and Fig. 4 to 8 show the corresponding relationship between the shear force Q and the measured story deflection δ. Fig. 11 a), 12 a) and 13 a) show the Q-δ curves obtained from the reversed repeated loading tests for series F in which the constant amplitude of the member rotation R were ± 0.01 rad.

Observed deformation mechanisms

Flexural story deflection δ_{fl} may be obtained by the integration of the curvature distributions of the specimens measured by the attached dial gages. Shear story deflection δ_{sh} and shear strain $\gamma(Q)$ are defined by the following equations respectively.

$$\delta_{sh} = \delta - \delta_{fl}, \quad \text{and} \quad \gamma(Q) = \delta_{sh}/2a$$

In the case of the specimen with small shear span ratio, it was recognized that the experimental curves were well agreed with those calculated by the next equation before the diagonal cracks appeared.

$$(Q) = 8Q/7Bd \cdot G_c \qquad G_c = \frac{E_c}{2(1+\nu)}$$

Fig. 9 and 10 show the results of the separation between flexural and shear deformation for the specimens subjected to the monotonous loading. Also Fig. 11 c), 12 c) and 13 c) show the similar results for the specimens subjected to the reversed repeated loading.

Although the employed method of curvature measuring is not so correct, remainders from the flexural deformation are large in the case of specimens with small shear span ratios.

Fig. 14 a), 15 a) and 16 a) show the changes of strain distribution of longitudinal reinforcing steels for the F-series specimens, where the strains at the completion of axial load transferring are defined zero. Also Fig. 14 b), 15 b) and 16 b) show the changes of strain distribution of lateral shear reinforcements.

PROPOSED DEFORMATION MODEL FOR THE ANALYTICAL METHOD

This model shown in Fig. 17 represents the column deformation as the sum of the rigid body rotation for flexure and shear distortion respectively. It may be considered that the reinforced concrete prisms 2 d_c x B assumed in the compressive and tensile zones of the column may act the moment resisting role in flexure and have the simplified hysteresis rule between the axial force and the average strain as shown in Fig. 18.

Assuming that the distributions of the axial forces T_t and T_c acted to these prisms are linear and the plane section is remained plane after deformation, the concentrated displacements Δ_{top} and Δ_{bottom} may be obtained by the numerical integration of the strain distributions. Increases of the displacements due to the slippage of the longitudinal reinforcing bars are discarded in the present analysis but these may be taken into account for changing the assumption on the force distributions in the prisms.

Actual numerical computation may be carried out on the simplified model with the divided prism elements as shown in Fig. 19.

Therefore, the depth of rotation centers of the critical section in the n-th incremental stage of load may be expressed by the following equation.

$$Y^n = \left(\frac{\Delta^n_{top}}{\Delta^n_{top} - \Delta^n_{bottom}} \right)(D - 2\cdot d_c) + d_c \qquad (1)$$

Neglecting the tensile stress of concrete but considering all the compressive stress of the concrete above Y, the equivalence conditions about the axial force N and the moment M of the column are expressed as follos, referring to Fig. 19.

a) After crack development in the critical section

$$N^n = T^n_{u1} + \frac{1}{2}(y - d_c)\cdot B\cdot\sigma^n_t + T^n_{L1} \qquad (2)$$

$$M^n = (T^n_{u1} - T^n_{L1})\cdot \frac{D-2dc}{2} + \frac{1}{2}(y-dc)\cdot B\cdot\sigma^n_t\cdot\frac{(3D-10d_c-2y)}{6} \qquad (3)$$

b) Before crack development in the critical section.

$$N^n = T^n_{u1} + \frac{1}{2}(\sigma^n_t + \sigma^n_b)(D-4d_c)B + T^n_{L1} \qquad (2)'$$

$$M^n = (T^n_{u1} - T^n_{L1})\frac{D-2dc}{2} + \frac{1}{2}(\sigma^n_t - \sigma^n_b)(D-4d_c)\cdot B\cdot\frac{1}{6}(D-4d_c) \qquad (3)'$$

shear force equivalence is

$$Q^n = \frac{M^n}{a} = \tau^n\cdot B\cdot y^n + \alpha\cdot\sum \sigma^n_{sv}\cdot A_v \qquad (4)$$

α : Effective coefficient of shear reinforcement

Any failure criterion of concrete under combined stress should be considered.

Total story deflection is as prescribed.

$$\delta^n = \delta^n_{f1} + \delta^n_{sh} = \left[\frac{\Delta^n_{top} - \Delta^n_{bottom}}{D - 2d_c} + \gamma^n(Q)\right]2a \qquad (5)$$

Succesive incremental calculation to the whole process produces the n+1 -th story deflection $\delta^{n+1} = \delta^n + \Delta\delta^n$.

CALCULATED RESULTS OF PRESTORING FORCE CHARACTERISTICS OF A REINFORCED CONCRETE COLUMN

For an example the specific details of the columns specimen F2 was given to the numeric calculation. The reinforced concrete prisms in the compressive and tensile zones of the column have the bredth B = 15cm and the depth $2d_c$ = 5.1cm. Both prisms are divided into four equal elements over the half distance of the story height. The reinforcing bars considered are 2-deformed bars of nominal diameter 19mm. The compressive strength f_c' and tensile one f_{sp} of concrete are 329 kg/cm^2 and 26.3kg/cm^2 respectively. The yield stress of the reinforcing bars is $\pm$ 4600 kg/cm^2. In present example the shear force effects for the column and the failure criterion of concrete under combined stress are dismissed but these factors may be easily considered in the analysis using the experimentally obtained results. Obtained hysteresis loop on the restoring force characteristics of reinforced concrete column is shown in Fig. 20. It is supposed that the difference between the experiment and analysis is caused by omitting the shear force effects.

SUMMARY

The deformations of the reinforced concrete columns under combined shear and flexure cannot be estimated only by flexural deformation. The correct solution to this problem may be achieved by taking account for the three deformation factors, i.e. conventional flexural deformation, the deformation due to the slippage of the longitudinal reinforcement and the shear distortion. This study shows an analytical method to estimate the column deformation, accompanying with the supporting experimental results.

RESUME

Les déformations des colonnes en béton armé soumises à des efforts combinés de cisaillement et de flexion ne peuvent pas être déterminées en ne tenant compte que des déformations dues à la flexion. La solution correcte de ce problème peut être obtenue en considérant les trois facteurs de déformation suivants: les déformations dues à la flexion, celles résultant du glissement des armatures longitudinales et celles dues au cisaillement. Cette étude présente une méthode analytique pour calculer les déformations de la colonne ainsi que les résultats d'essais.

ZUSAMMENFASSUNG

Die Deformation von Stahlbetonstützen unter kombiniertem Schub und Biegung kann nicht allein nur aus der Biegedeformation geschätzt werden. Die korrekte Lösung des Problems lässt sich durch Berücksichtigung der drei Deformationsfaktoren gewinnen: übliche Biege-Deformation, Deformation infolge Schlupf der Längseisen und infolge Schub. Diese Studie zeigt eine analytische Methode zur Abschätzung der Säulendeformation und die bestätigenden experimentellen Resultate.

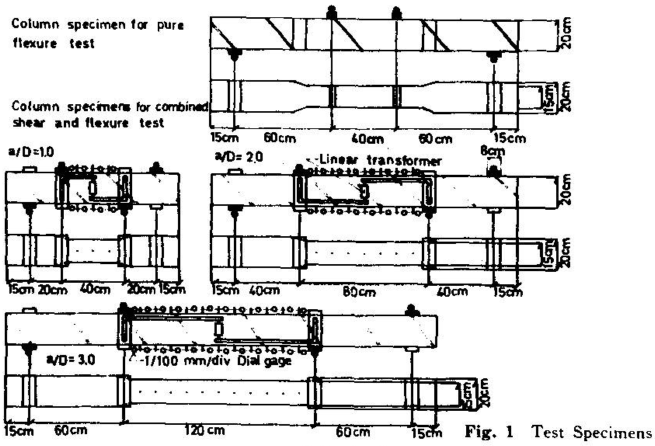

Fig. 1 Test Specimens

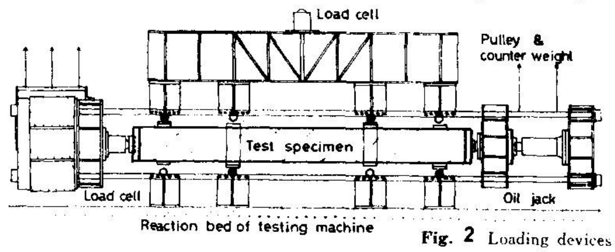

Fig. 2 Loading devices

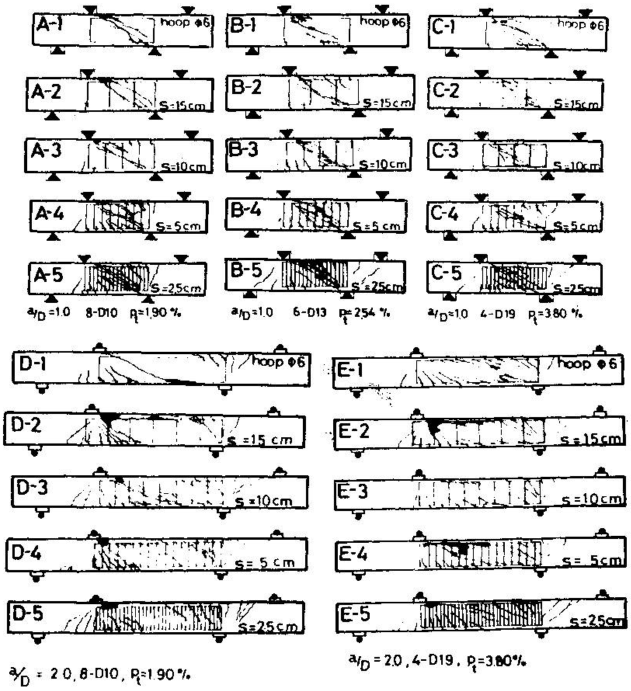

Fig. 3 Cracks of specimens at failure

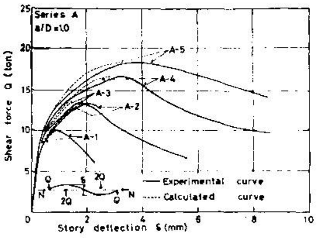

Fig. 4 Relationships between the shear force and the story deflection ($a/D=1.0$, $p_t=1.90\%$)

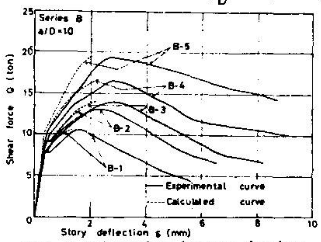

Fig. 5 Relationships between the shear force and the story deflection ($a/D=1.0$, $p_t=2.54\%$)

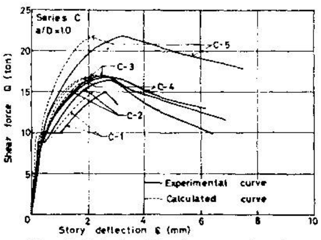

Fig. 6 Relationships between the shear force and the story deflection ($a/D=1.0$, $p_t=3.80\%$)

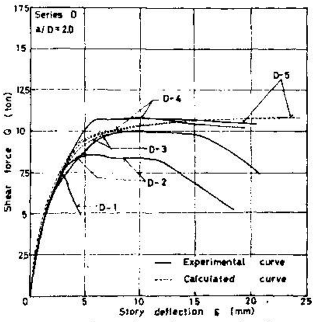

Fig. 7 Relationships between the shear force and the story deflection ($a/D=2.0$, $p_t=1.90\%$)

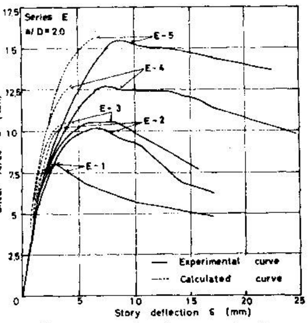

Fig. 8 Relationships between the shear force and the story deflection ($a/D=2.0$, $p_t=3.80\%$)

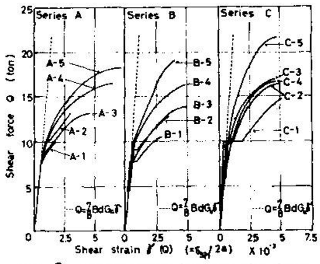

Fig. 9 Relationships between the shear force and the shear strain ($a/D=1.0$)

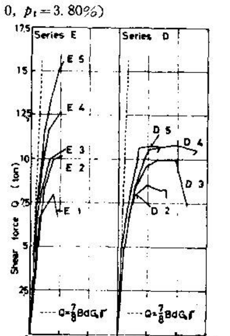

Fig. 10 Relationships between the shear force and the shear strain ($a/D=2.0$)

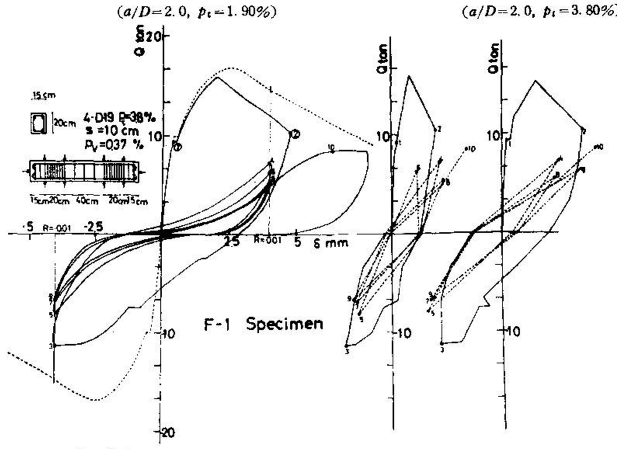

a) Q-δ curve b) Q-δ_{fl} curve c) Q-δ_{sh} curve

Fig. 11 Q-δ, Q-δ_{fl}, Q-δ_{sh} curves of F-1 specimen ($a/D=1.0$)

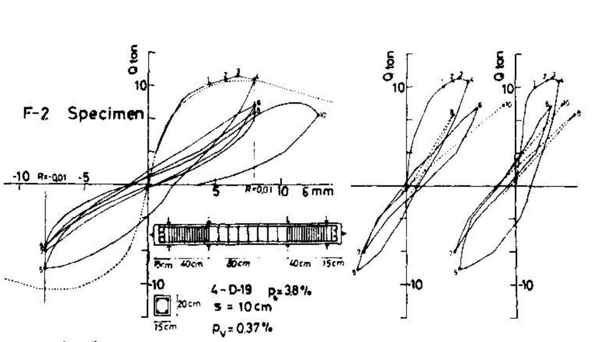

a) Q-δ curve b) Q-δ_{fl} curve c) Q-δ_{sh} curve

Fig. 12 Q-δ, Q-δ_{fl}, Q-δ_{sh} curves of F-2 specimen ($a/D=2.0$)

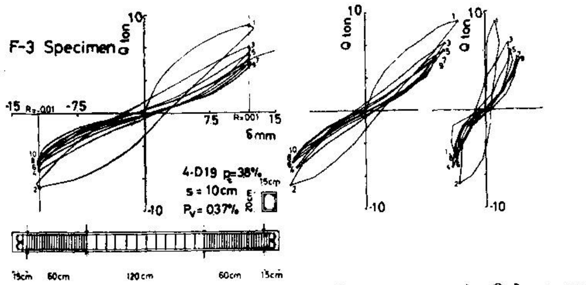

a) Q-δ curve b) Q-δ_{fl} curve c) Q-δ_{sh} curve

Fig. 13 Q-δ, Q-δ_{fl}, Q-δ_{sh} curves of F-3 specimen (a/D=3.0)

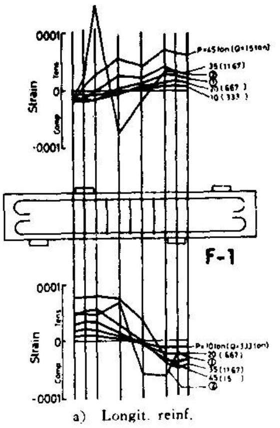

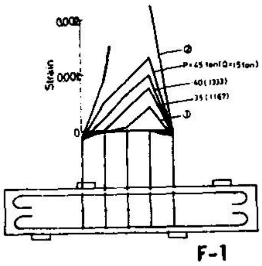

b) Lateral reinf.

Fig. 14 Strain distributions of lonfitudinal steels and lateral ones (a/D=1.0, p_t=3.80%, p_w=0.37%)

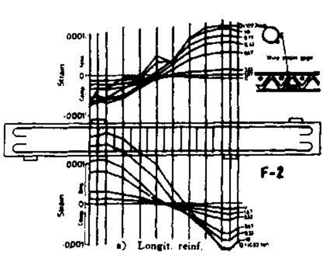

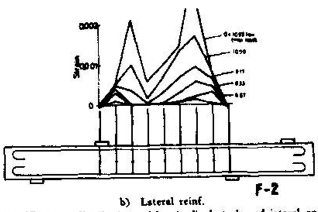

b) Lateral reinf.

Fig. 15 Strain distributions of longitudinal steels and lateral ones (a/D=2.0, p_t=3.80%, p_w=0.37%)

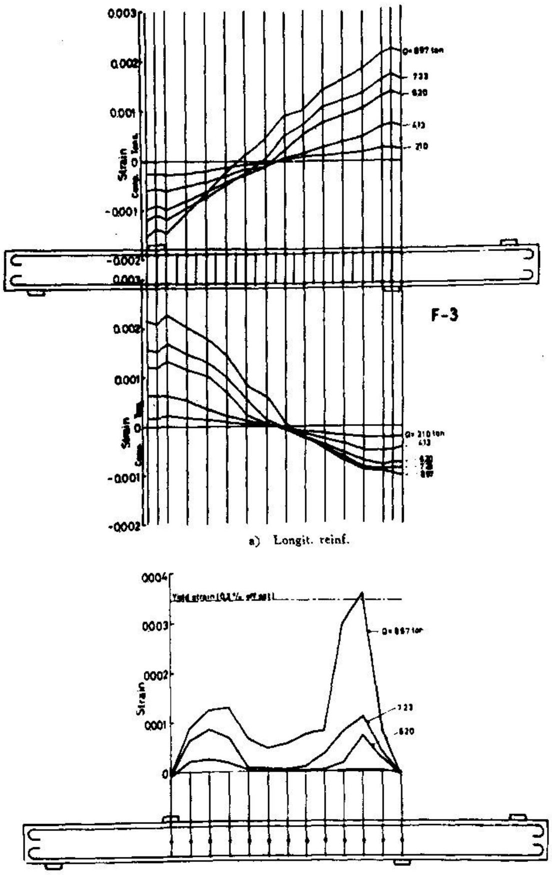

Fig. 16 Strain distributions of longitudinal steels and lateral ones (a/D=3.0, p_t=3.80%, p_w=0.37%)

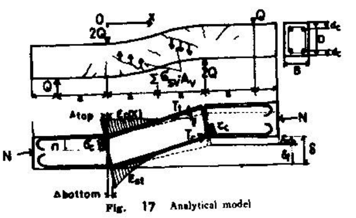

Fig. 17 Analytical model

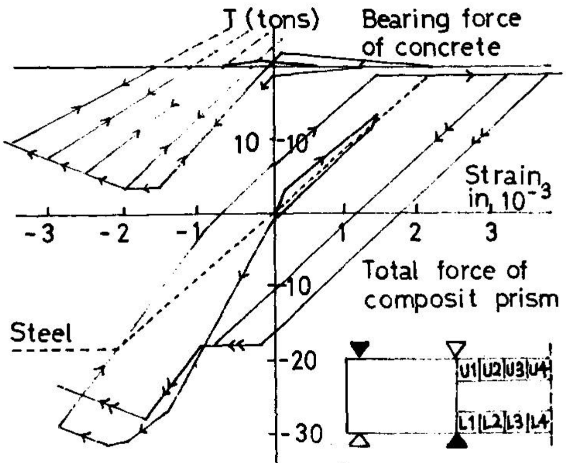

Fig. 18 Hysteresis rule

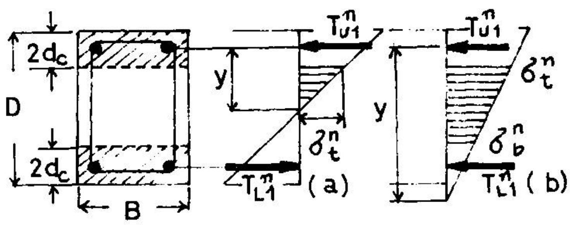

Fig. 19 Force equivalence of section

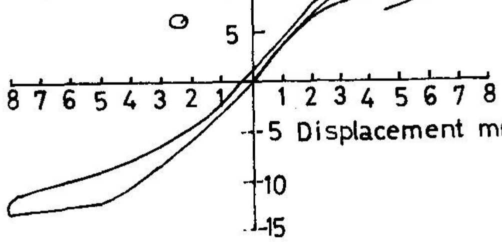

Fig. 20 Calculated hysteresis loop